Electrochemistry Communications 65 (2016) 44–47

Contents lists available at ScienceDirect

Electrochemistry Communications

journal homepage: www.elsevier.com/locate/elecom

Short communication

Origin of additional capacities in selenium-based ZnSe@C nanocomposite Li-ion battery electrodes

Yanhua Xu [a], Jianwen Liang [a], Kailong Zhang [a], Yongchun Zhu [a,*], Denghu Wei [b], Yitai Qian [a,*]

[a] Hefei National Laboratory for Physical Science at Microscale and Department of Chemistry, University of Science and Technology of China, Hefei, Anhui 230026, PR China
[b] School of Materials Science and Engineering, Liaocheng University, Liaocheng, Shandong 252000, PR China

ARTICLE INFO

Article history:
Received 28 December 2015
Received in revised form 2 February 2016
Accepted 10 February 2016
Available online 17 February 2016

Keywords:
ZnSe
Mesoporous nanospheres
Core-shell
Elemental selenium
Li-ion batteries

ABSTRACT

Metal sulfides/selenides (MS_x/MSe_x) are used as promising alternative electrode materials for Li-ion batteries. However, the performance of MS_x/MSe_x electrodes is often accompanied by rising and additional reversible capacities beyond their theoretical capacities during cycling, the mechanisms of which are still poorly understood. This study employs *ex situ* X-ray photoelectron spectroscopy, along with cyclic voltammetry to control the electrochemical charge/discharge process, to explore the origin of the additional capacities in ZnSe@C composite electrodes. Such ZnSe@C composites exhibit a rising reversible capacity of 960 mAh g^{-1} (approximately 2 times its theoretical capacity) at 0.2 A g^{-1} after 400 cycles at 0.01–3 V. The analysis shows that a major contribution to the extra rising capacity in this system is due to the generation and activation of Se during the electrochemical process.

1. Introduction

Various types of metal sulfide/selenide (MS_x/MSe_x) materials have been widely investigated as promising materials for Li-ion batteries (LIBs) because of their higher theoretical capacity compared with that of conventional graphite [1–7]. However, the use of MS_x/MSe_x materials is often accompanied by rising and additional reversible capacities over their theoretical capacities during consecutive cycles *via* a mechanism that is still poorly understood. A number of viewpoints have been proposed to explain such phenomena, such as interfacial lithium storage and the formation of a 'polymer/gel-like film' [1,8].

Herein, we focus on ZnSe materials due to their suitable theoretical capacity of approx. 557 mAh g^{-1} [9] and the large difference in electrochemical oxidation/reduction potential between zinc and selenium. Xue was the first to suggest the use of ZnSe as an anode material for LIBs and proposed the conversion (ZnSe ↔ Zn) and alloying (Zn ↔ Li_xZn) storage mechanisms of ZnSe in the lithiation/delithiation process [10]. Zhang reported on sphere-like ZnSe and ZnSe-rGO nanocomposites as anode materials that showed attractive cycling performances [11,12]. Furthermore, Kwon prepared ZnSe/C nanoparticles and used *ex situ* X-ray diffraction and extended X-ray absorption fine structure analyses to verify the detailed reaction mechanism [9]. Both Zhang and Kwon found that the composites exhibited rising reversible capacities in consecutive cycles, but the reasons were not clear.

In this work, we demonstrate the use of a ZnSe@C composite anode material with a rising reversible capacity of 960 mAh g^{-1} at 0.2 A g^{-1} after 400 cycles at 0.01–3 V. *Ex situ* XPS and CV, which facilitated control over the electrochemical charge/discharge process, were employed to investigate the origin of the additional capacities in the ZnSe@C composite electrode. The analysis shows that the generated and activated Se makes a major contribution to the extra rising capacity in this system during the electrochemical process. These results implicate significant electrochemical activation and storage mechanisms in a wider range of nanocomposites used in LIBs.

2. Experimental procedure

Typically, 0.372 g $ZnNO_3 \cdot 6H_2O$ and 0.146 g hexadecyltrimethylammonium bromide were dissolved in 20 mL water. Subsequently, 0.216 g Na_2SeO_3, 3 mL $NH_3 \cdot H_2O$ and 5 mL $N_2H_4 \cdot H_2O$ were added to form a solution. After stirring transparent, the solution was loaded into a 50-mL Teflon-lined stainless-steel autoclave and maintained at 180 °C for 10 h. The ZnSe precursor was washed with distilled water and drying in a vacuum oven. ZnSe@C composites were prepared by thermal annealing of acetylene with ZnSe precursor at 450 °C for 10 h. The reactor atmosphere was under a continuous flow of acetylene diluted with purified argon gas (1:9, $V_{acetylene}/V_{argon}$) at a heating rate of 3 °C min^{-1}.

Phase characterization was performed by X-ray powder diffraction (XRD, Philips X'pert X-ray diffractometer, Cu Ka radiation, λ = 1.54182 Å) and Raman spectroscopy (JYLABRAM-HR Confocal Laser Micro-Raman spectrometer at 514.5 nm). Microstructure and

* Corresponding authors. Tel.: +86 551 360 1589; fax: +86 551 360 7402.
E-mail addresses: ychzhu@ustc.edu.cn (Y. Zhu), ytqian@ustc.edu.cn (Y. Qian).

http://dx.doi.org/10.1016/j.elecom.2016.02.009
1388-2481/

morphology characterization was determined by transmission electron microscopy (TEM, H7650), high-resolution transmission electron microscopy (HRTEM, JEOL 2010) and scanning electron microscopy (SEM, EOL-JSM-6700F, 20KV). The carbon content was determined by elemental analysis (Elemental vario EL cube). BET surface area and pore size distribution were measured on a Micromeritics ASAP 2020 accelerated surface area and porosimetry system.

CR 2016 coin-type half cells were assembled for evaluating the electrochemical performance. The working electrode was made using 70 wt.% active material, 20 wt.% carbon black and 10 wt.% carboxymethyl cellulose binder on a current collector of copper foil. The ZnSe@C loading was approximately 2.0 mg cm^{-2}. The 2016 coin cells were assembled with Li foil as the counter electrode, celgard 2400 as the separator, and a 1.0 M $LiPF_6$ solution of EC/DEC (1:1, v/v) as the electrolyte.

3. Results and discussion

The XRD patterns (Fig. 1a) of the prepared materials show evidence of diffraction peaks at 27.4, 45.5 and 53.9°, which can be indexed to the (111), (220) and (311) crystal planes of cubic ZnSe (JCPDS 80-0021), respectively. The Raman spectrum of the ZnSe@C composite exhibited typical carbon peaks at 1344 (D-band of carbon) and 1592 cm^{-1} (G-band of carbon). In addition, the carbon content of the ZnSe@C was determined to be approximately 16.7 wt.%.

The nanospherical structure of ZnSe@C was revealed by SEM and TEM (Fig. 1d and e). As shown in the higher magnification SEM image (Fig. 1d inset), it was found that the ZnSe@C nanoparticles aggregated into nanospheres. HRTEM further revealed a uniform carbon coating shell with a thickness of 3 nm. To obtain further information about these core-shell structures, the ZnSe@C composites were treated with 10 mL 1 M HCl for 6 h at room temperature (Fig. 1e inset). The N_2 adsorption–desorption isotherm and the BJH pore distribution revealed the mesopores (~20 nm) in the resulting ZnSe@C materials (Fig. 1c), with a surface area of 38.6 m^2 g^{-1}.

Cyclic voltammograms (CVs) of the ZnSe@C electrode were evaluated at a scanning rate of 0.1 mV s^{-1} over the potential range of 3 to 0.01 V (Fig. 2a). In the first cycle, a fairly minor peak at 0.8 V was assigned to SEI layer formation, while the relatively broad peak at 0.3 V corresponds to various Li_xZn alloy phases [11]. In the charging process, the small peak at 0.5 V was attributed to de-alloying of Li–Zn, while the peak at 1.3 V was assigned to the transformation of ZnSe from Li_2Se and Zn [9]. In the two scanning cycles that followed, the oxidation peaks overlapped with one another, indicating the reversible electrochemical reactions of the ZnSe. The reduction peaks turned into a weak peak at approximately 0.5 V and a main peak at 0.75 V, which is believed to be associated with the reversible reduction of the Zn metal [9,10]. During the second cycle of the charging process, a very weak broad peak near 2.5 V was detected (inset picture), which can be attributed to oxidation of Li_2Se to elemental Se (an illustration will be given in the following discussion).

Fig. 2b shows the charge/discharge profiles of ZnSe@C at 0.2 A g^{-1} for the 10th, 200th and 400th cycles (0.01–3 V). It can be seen that the capacity increased. Fig. 2c shows the rate performance of ZnSe@C with different specific currents for 10 cycles (0.01–3 V, 0.01–1.75 V). It can be seen that the capacity of ZnSe@C increased at an abnormal rate from the second cycle at 0.1, 0.2, and 0.5 A g^{-1}, while remaining stable until 2 A g^{-1} (0.01–3 V). Meanwhile, when the charging voltage was adjusted to 1.75 V, the capacity of the ZnSe@C electrode gradually decreased. Fig. 2d depicts the capacity of the ZnSe@C electrode with different charging processes at 0.2 A g^{-1} for 400 cycles. When charged to 3 V, the capacity of the ZnSe@C electrode rose slowly in subsequent cycles. At the end of the 400th cycle, a reversible capacity as high as 960 mAh g^{-1} was obtained. The SEM image after 100 cycles is present in Fig. 2d (inset), and spheres are basically maintained.

The reversible capacity of ZnSe@C increased to a higher value than the theoretical capacity. Such a capacity rise with cycling is common for various nanostructured metal oxide/sulfide electrodes. Maier and Lou suggested that such behavior could be attributed to the reversible formation and decomposition of an organic polymeric/gel-like film coating originating from the electrolyte around the active materials at low voltage, which could supply interfacial storage for additional Li-ions by a so-called "pseudo-capacitance-type behavior" [13–15].

Therefore, to probe the relationship between capacity and pseudocapacity, CV measurements of ZnSe@C were obtained at different scan rates. The anodic peak currents of ZnSe@C after 200 cycles as a function of sweep rate are shown in Fig. 3a. The sweep rate and the current obey a power-law relationship indicated by $i = av^b$. For surface-controlled electrochemical processes, the b-value should approach 1 [16,17]. However, when the charge storage occurs in the

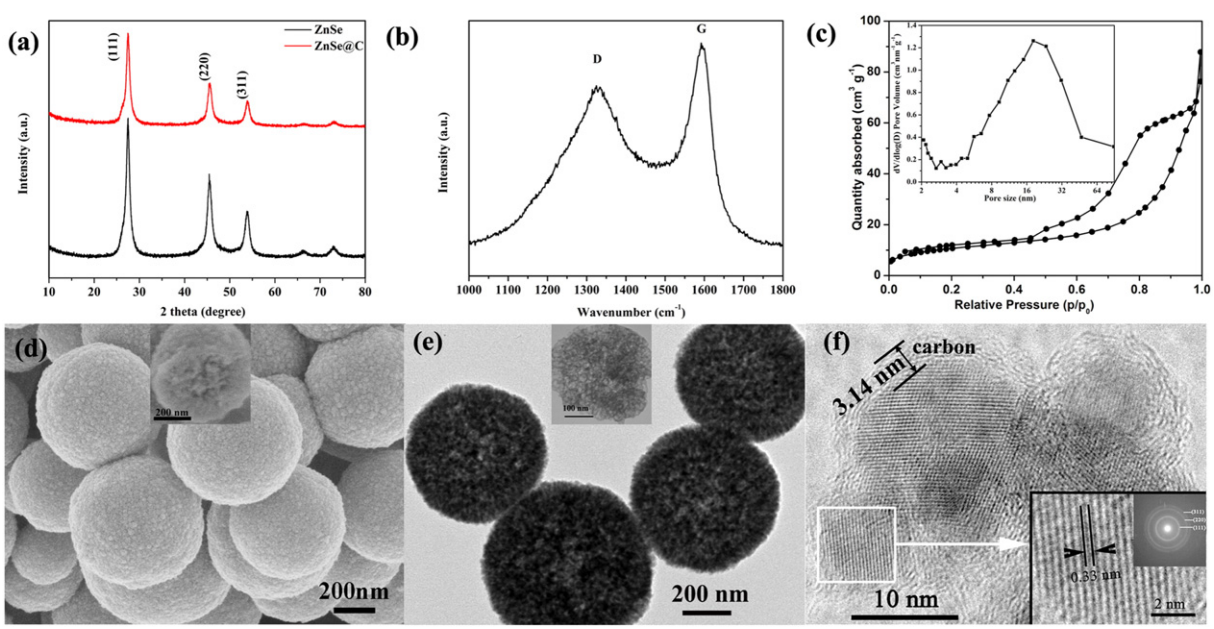

Fig. 1. (a) XRD pattern of ZnSe and ZnSe@C; (b) Raman spectrum of the ZnSe@C composite; (c) N_2 adsorption–desorption isotherm and pore size distribution of ZnSe@C composite; (d) SEM, (e) TEM, and (f) HRTEM images of ZnSe@C composite.